Polymer Journal (2018) 50:455–465
https://doi.org/10.1038/s41428-018-0034-x

ORIGINAL ARTICLE

Light-driven molecular switching of atropisomeric polymers containing azo-binaphthyl groups in their side chains

Fathy Hassan[1,2] · Takafumi Sassa[3] · Takuji Hirose[2] · Yoshihiro Ito[1,4] · Masuki Kawamoto[1,2,4,5]

Received: 25 December 2017 / Revised: 5 February 2018 / Accepted: 8 February 2018 / Published online: 14 March 2018

Abstract

Light-driven atropisomeric polymers containing azo and binaphthyl units with a conjugated structure were designed and synthesized. The polymers exhibit a glass transition temperature higher than 75 °C with thermal stability above 280 °C and form uniform and smooth thin films without grain boundaries. The *trans-cis* isomerization is efficiently reversible upon alternating photoirradiation with UV and visible light or with heat. The photoisomerization of the chiral polymer results in photomodulation of the ellipticity and optical rotation ($[\alpha]_D^{25}$), owing to a chiroptical switching behavior. The maximum changes in the dihedral angle and $[\alpha]_D^{25}$ are 21% and 700°, respectively, from the initial state owing to a photoinduced molecular twisting motion of the binaphthyl moiety. The polymer also displays photoswitchable fluorescence with a maximum at 409 nm. A photoinduced change in the refractive index of the formed film is also observed after irradiation with linearly polarized light at 532 nm according to the anisotropic molecular orientation. These results suggest that atropisomeric polymers are potential candidates for light-driven chiroptical switches.

Introduction

Light-driven molecular switches are important technologies for future photonics applications [1]. They provide opportunities for the development of smart devices with the possibility of miniaturization [2, 3] and are designed by the incorporation of photoswitching into chiral molecules. To perform these functions, materials show reversible changes between two different states, which can be efficiently interchanged by incident light, where a high sensitivity and fast response are required [4].

A typical photoswitching molecule is azobenzene (AB), which is a well-known photochromic compound. AB exhibits reversible changes upon photoirradiation with UV/visible light (Vis) or heat [5]. These changes include changes in the molecular shape, length, orientation and dipole moment (δ) owing to *trans-cis* isomerization (Scheme 1(a)). AB possesses a rod-like shape in the *trans* form ($\delta = 0$ Debye), while the *cis* isomer is bent ($\delta = 3$ Debye). The distance between the 4- and 4′-carbons at the para positions decreases from 9.0 Å (*trans* form) to 5.5 Å (*cis* form) [6]. The photoinduced change in the molecular orientation results in the *trans* form changing its orientation to be perpendicular to the polarization direction of the actinic light after multiple cycles of isomerization, which is known as the Weigert effect [7]. For the chiral characteristic, the 1,1′-binaphthyl (BN) skeleton acts as an axially chiral segment [8]. The BN moiety undergoes a change in the dihedral angle (θ) between the two naphthalene rings owing to the restricted rotation around the

Electronic supplementary material The online version of this article (https://doi.org/10.1038/s41428-018-0034-x) contains supplementary material, which is available to authorized users.

✉ Yoshihiro Ito
y-ito@riken.jp

✉ Masuki Kawamoto
mkawamot@riken.jp

[1] Emergent Bioengineering Materials Research Team, RIKEN Center for Emergent Matter Science, 2-1 Hirosawa, Wako, Saitama 351-0198, Japan

[2] Graduate School of Science and Engineering, Saitama University, 255 Shimo-Okubo, Sakura-ku, Saitama 338-8570, Japan

[3] Photonics Control Technology Team, RIKEN Center for Advanced Photonics, 2-1 Hirosawa, Wako, Saitama 351-0198, Japan

[4] Nano Medical Engineering Laboratory, RIKEN, 2-1 Hirosawa, Wako, Saitama 351-0198, Japan

[5] Photocatalysis International Research Center, Tokyo University of Science, 2641 Yamazaki, Noda, Chiba 278-8510, Japan

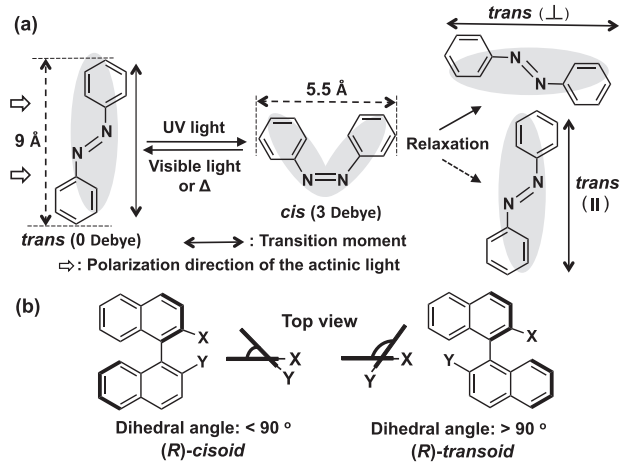

Scheme 1 **a** Photo-induced change in molecular structure of azobenzene moiety, (**b**) change in dihedral angle of binaphthyl moiety

naphthalene–naphthalene bond (Scheme 1(b)), which results in the two configurations of *cisoid* ($\theta < 90°$) and *transoid* ($\theta > 90°$) [9].

The combination of AB and BN units in a single molecule leads to novel optical properties. Montbach et al. introduced two AB units with ether linkages at the para positions to the 2,2′-positions of BN and fabricated fixable optically addressed photochiral displays with nematic liquid crystals for the first time [10]. Replacing the terminal ether groups with ester units possessing an extended π conjugation resulted in the self-organization of the AB-BN-AB into an optically tunable helical superstructure, which led to a reversible light-directed reflection in the near-infrared region [11]. When two AB units were incorporated at the 5,5′-positions of BN, distinct phase-induced chiral and photoswitching properties of the cholesteric liquid crystals were observed [12]. Enantiomeric chiral dopants composed of BN connected to AB through the 6,6′-positions in the liquid crystal showed reversible and fast red, green, and blue (RGB) reflections in the cell [13].

Kawamoto et al. introduced nitro AB segments into an ether BN unit, and the resulting compound was a novel chiral amorphous molecular material that exhibited highly efficient photoinduced polarization rotations [14]. They also designed non-destructive erasable molecular switches by connecting AB and BN moieties through an alkyl chain in the macrocycle structure and showed a uniquely chiroptical switching behavior with high fatigue resistance [15, 16]. However, the dynamic molecular motion was not efficient owing to relaxation because the AB and BN moieties were connected by a flexible alkyl chain. In addition, aggregation occurred in the case of small molecules owing to the phase separation, and it was difficult to form a homogeneous thin film. To overcome these problems, in this study, new atropisomeric polymers composed of AB and BN were

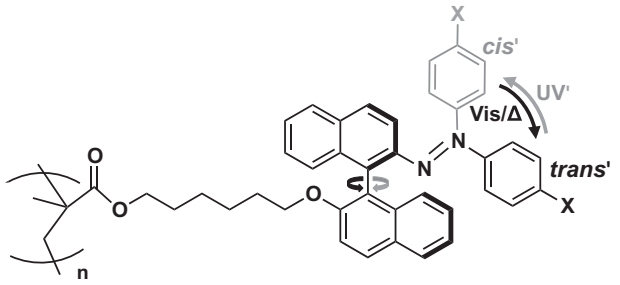

Scheme 2 Molecular structure of the light-driven atropisomeric azo polymer

designed and synthesized (Scheme 2). An AB moiety was directly connected to a BN moiety in the side chains. The rigid chromophore was expected to enable direct control over the molecular structure without relaxation. Additionally, to avoid the molecular aggregation that occurs in the case of small molecules, the AB and BN units were incorporated into the polymeric structure in the side chains, separated by ethylenic bridges. The polymeric material facilitated the formation of uniform and smooth thin films owing to the high molar mass and high solubility, which are useful for various device fabrications.

Experimental procedures

Materials

Unless otherwise noted, all chemicals and solvents were purchased from commercial suppliers and were used as received without further purification. Racemic 1,1′-bi-2-naphthol, 4-nitroaniline, nitrosobenzene, *N*-benzylcinchonidinium chloride, 6-bromo-1-hexanol, potassium peroxymonosulfate, methacryloyl chloride, and potassium carbonate were purchased from Tokyo Chemical Industry Co., Ltd. (Tokyo, Japan). Anhydrous *N*,*N*-dimethylformamide (DMF), anhydrous dimethyl sulfoxide (DMSO), anhydrous acetone, n-hexane, ethyl acetate, chloroform, methanol, tetrahydrofuran (THF, spectroscopic grade), and 1,4-dioxane (spectroscopic grade) were purchased from Wako Pure Chemicals Industries Ltd. (Osaka, Japan). 2,2′-Azobisisobutyronitrile (AIBN), triethylamine, hydroquinone, ammonium sulfite monohydrate, ammonia solution ($NH_{3\ aq.}$, 28%), sodium hydroxide, acetic acid, hydrochloric acid (1 N), sodium sulfate, anhydrous magnesium sulfate, benzene, and isopropanol were purchased from Junsei Chemical Co., Ltd. (Tokyo, Japan). Deuterated chloroform and deuterated 1,4-dioxane were purchased from Cambridge Isotope Laboratories (Tewksbury, MA, USA). A fused silica substrate was purchased from Matsunami Glass Ind. Ltd. (45 mm × 12 mm, thickness: 1 mm, Osaka, Japan).

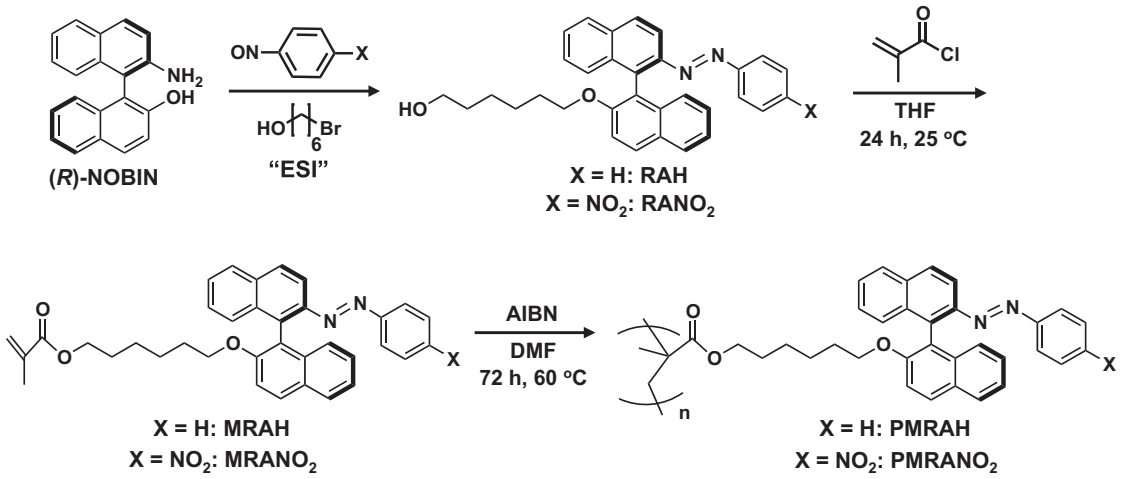

Scheme 3 Synthetic pathway for **PMRAH** and **PMRANO$_2$**

Synthesis of the atropisomeric azo monomers

Scheme 3 shows the synthetic route for the atropisomeric azo polymers. The atropisomeric unit, 2-amino-2′-hydroxy-1,1′-binaphthyl ((*R*)-NOBIN), was synthesized according to a previously reported method [17, 18]. (*R*)-NOBIN was separated by its optical resolution with >99% enantiomeric excess ($[\alpha]_D^{25}$: +124, $c = 1.0$ in THF). The reaction of (*R*)-NOBIN with 1.2 equiv. of aryl nitroso species yielded the atropisomeric azo compounds: **RAH** when $X = H$ and **RANO$_2$** when $X = NO_2$. After free radical polymerization of the methacrylated monomer under deoxygenated conditions, the colored powder of the polymer was obtained by precipitation in methanol.

The methacrylated monomer of **RAH** (**MRAH**) was synthesized as follows. Triethylamine (0.4 g, 4.2 mmol) and hydroquinone (5 mg, 0.05 mmol) were added to a solution of **RAH** (1.0 g, 2.1 mmol) in THF (50 mL). After the reaction solution was stirred at 0 °C for 10 min, methacryloyl chloride (0.3 g, 2.3 mmol) in THF (10 mL) was slowly added to the solution. The reaction mixture was gradually warmed to 25 °C and then stirred for 24 h under argon. The resulting mixture was quenched by distilled water (250 mL). The crude product was extracted with dichloromethane (300 mL) before drying over $MgSO_4$. The solvent was evaporated under reduced pressure, and the oily residue was purified by column chromatography on silica gel (eluents: hexane:ethyl acetate = 90:10 v/v) and by size exclusion chromatography (eluent: chloroform) to afford **MRAH** (0.7 g, 65%) as an orange-red oil. ^{1}H-NMR (300 MHz, $CDCl_3$): $\delta = 0.80$–1.01 (m, 4 H, binaphthyl–O–$CH_2CH_2CH_2CH_2CH_2CH_2OCOC(CH_2CH_3)$), 1.25–1.37 (m, 4 H, binaphthyl-O–$CH_2CH_2CH_2CH_2CH_2CH_2OCOC(CH_2CH_3)$), 1.94 (s, 3 H, binaphthyl–O–$CH_2CH_2CH_2CH_2CH_2CH_2OCOC(CH_2CH_3)$), 3.85–3.97 (m, 4 H, binaphthyl–O–$CH_2CH_2CH_2CH_2CH_2CH_2OCOC(CH_2CH_3)$), 5.54 (s, 1 H, binaphthyl–O–$CH_2CH_2CH_2CH_2CH_2CH_2OCOC(CH_2CH_3)$), 6.07 (s, 1 H, binaphthyl–O–$CH_2CH_2CH_2CH_2CH_2CH_2OCOC(CH_2CH_3)$), 7.18–7.19 (m, 2 H, aromatic ring), 7.27–7.35 (m, 5 H, aromatic ring), 7.40–7.55 (m, 5 H, aromatic ring), 7.88–7.91 (d, 1 H, $J = 8.1$ Hz, aromatic ring), 7.95–8.03 (m, 3 H, aromatic ring), 8.15–8.18 (d, 1 H, $J = 8.7$ Hz, aromatic ring); ^{13}C-NMR (300 MHz, $CDCl_3$): $\delta = 18.31$, 25.16, 25.24, 28.22, 29.08, 64.52, 69.24, 114.56, 115.02, 120.94, 122.81, 123.38, 125.09, 125.84, 126.28, 126.48, 127.26, 127.31, 127.72, 128.12, 128.75, 128.79, 129.44, 130.41, 133.72, 134.49, 134.89, 136.50, 136.89, 147.98, 152.78, 154.52, 167.41; FT-IR (ν cm^{-1}): 3100, 3000, 2950, 2850, 1750, 1600, 1450, 1400, 1350, 1200, 1000, 900, 720, 675, 650; Anal. calcd. for $C_{36}H_{34}N_2O_3$: C, 79.68; H, 6.32; N, 5.16. Found: C, 79.52; H, 6.38; N, 5.02; HRMS calcd. for $C_{36}H_{34}N_2O_3$ $[M + Na]^+$: 565.2462, found: 565.2462.

MRANO$_2$ was synthesized using a method similar to that used for the synthesis of **MRHA**. Yield: 67%; Anal. calcd. for $C_{36}H_{33}N_3O_5$: C, 73.58; H, 5.66; N, 7.15. Found: C, 73.58; H, 5.78; N, 6.87; HRMS calcd. for $C_{36}H_{33}N_3O_5$ $[M + Na]^+$: 610.2312, found: 610.2312.

Polymerization

The polymer of **MRAH** (**PMRAH**) was synthesized as follows. AIBN (8.2 mg, 0.05 mmol) was added to a solution of **MRAH** (0.54 g, 1.0 mmol) in anhydrous DMF (10 mL) under argon. The reaction solution was degassed by freeze-pump-thaw cycles three times and then stirred for 72 h at 60 °C. The solution was poured into methanol (100 mL) after cooling to 25 °C. The precipitated product was collected by filtration. After the solid residue was dissolved in chloroform, the resulting solution was precipitated in methanol

Table 1 The characteristics of the atropisomeric azo polymers

	M_n	M_w	M_w/M_n	$[\alpha]_D^{25}$	T_{10} (°C)	T_g (°C)
PMRAH	7030	14,100	2.00	+255	288	77
PMRANO$_2$	7960	11,600	1.50	+138	325	112

twice to afford **PMRAH** as an orange-red powder (0.3 g, 55%). The number-average molecular weight (M_n) was 7030; the polydispersity (weight-average molecular weight (M_w)/M_n) was 2.0.

Another polymer of **MRANO$_2$** (**PMRANO$_2$**) was synthesized by free-radical polymerization with **MRANO$_2$** in a similar manner. Yield: 52%; M_n: 7960; M_w/M_n: 1.5.

Thermal analysis

The thermal properties were evaluated using thermogravimetric analysis (TGA; TGA-50, heating rate: 10 °C min^{-1} under nitrogen; Shimadzu Co. Ltd., Kyoto, Japan) and differential scanning calorimetry (DSC; SII NanoTechnology EXSTAR 6220, heating and cooling rate: 10 °C min^{-1} under nitrogen; Seiko Instruments Inc., Tokyo, Japan).

Spectroscopic measurements

The photoresponsive behavior was studied using UV-Vis absorption spectroscopy (V-550, JASCO Co. Ltd., Tokyo, Japan). The thermal back-isomerization was examined on the same spectrometer equipped with a temperature controller system (EHC-477, JASCO). Photoluminescence spectra were recorded using a spectrofluorometer (FP-6500, JASCO). Circular dichroism (CD) spectra were obtained using a CD spectrophotometer (J-720, JASCO). Optical rotation was determined using a polarimeter (P-2200, path length: 10 cm, solvent: THF; JASCO). Samples were irradiated at 365 nm (light intensity: 5 mW/cm^2) and 436 nm (light intensity: 3 mW/cm^2) using glass filters (HQBP365 and HQBP436, respectively, Asahi Spectra, Tokyo, Japan) and a 120 W high-pressure mercury lamp (REX-120, Asahi Spectra).

Results and discussion

Synthesis and characterization of the atropisomeric azo polymers

Table 1 shows the characteristics of the azo polymers. From the M_n and M_w/M_n values, it was calculated that these polymers possessed 14–20 atropisomeric units in the side chain. Optical rotation measurements revealed that the dextrorotatory nature was maintained after the modification

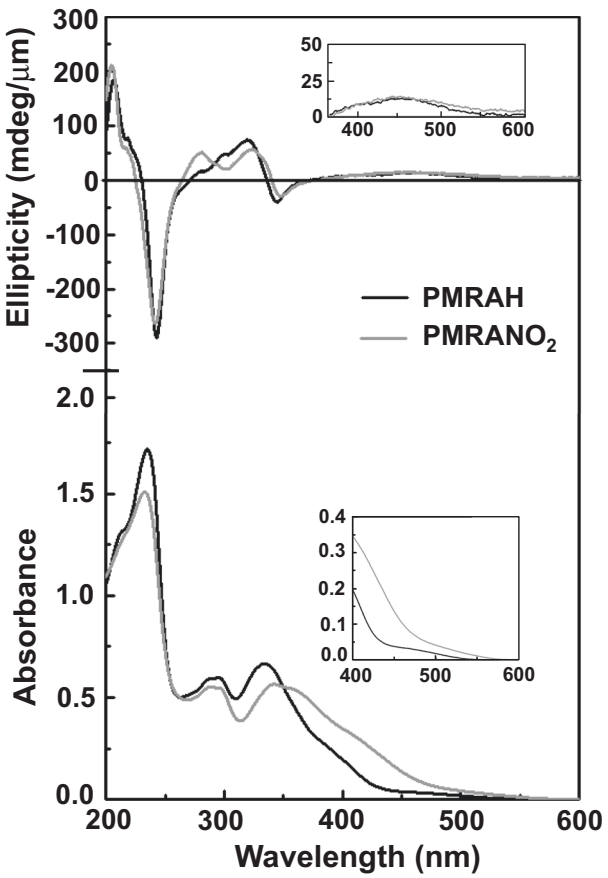

Fig. 1 Absorption and CD spectra for **PMRAH** and **PMRANO$_2$** neat films (film thickness = 135 and 120 nm), respectively

of (*R*)-NOBIN. These results suggested that the optical rotation of the atropisomeric unit arose from the axial chirality of the BN unit. The thermal behavior was investigated by TGA and DSC. TGA indicated that **PMRAH** and **PMRANO$_2$** had relatively high thermal stabilities with a weight loss of 10% at 288 and 325 °C (Fig. S1). We also detected endothermic events for **PMRAH** corresponding to a glass transition temperature (T_g) of 77 °C for the third cycle in the DSC measurements (Fig. S2). **PMRANO$_2$** exhibited a T_g of 112 °C, which indicated that the polymers were amorphous because of steric hindrance from the two non-planar naphthalene rings in the side chain. The thermal stability and amorphous nature are advantageous for solution-processed films.

The polymers formed uniform and smooth films on a fused silica substrate via spin-coating or drop-casting techniques (Fig. S3). The resulting films showed good transparency without grain boundaries. The film thickness could be controlled over a range from 30 nm to 4.5 μm by varying the concentration of the polymer solution. This flexible processability contributed to the fabrication of the nano- to micrometer-scale films (Fig. S4).

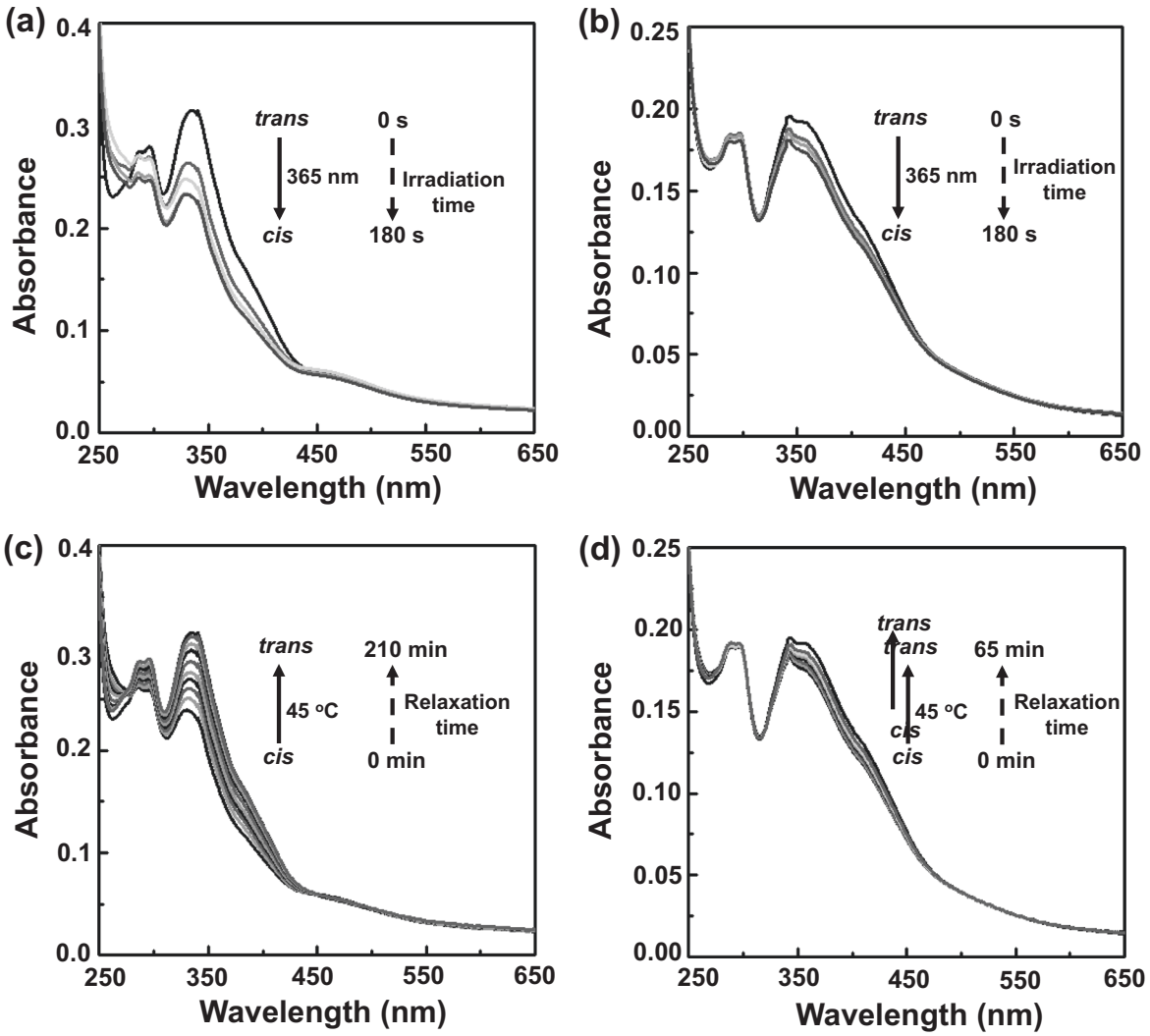

Fig. 2 Isomerization behavior of polymers neat films; (**a**) and (**b**) *trans* to *cis* photoisomerization after UV irradiation at 365 nm, (**c**) and (**d**) *cis* to *trans* thermal back isomerization at 45 °C for **PMRAH** and **PMRANO$_2$** (film thickness = 40 and 30 nm), respectively

Isomerization behavior of the atropisomeric azo polymers

Figure 1 shows the absorption and CD spectra of **PMRAH** and **PMRANO$_2$** in neat films (film thickness: 135 and 120 nm, respectively). The maximum absorption wavelengths (λ_{maxs}) were 234, 297, 341, and 350 nm. The λ_{maxs} of the polymers were similar to those of the BN moiety [19] and were attributed to the ^1B_b (234 nm), ^1L_a (297 nm), and ^1L_b (341 nm) transitions. The ^1B_b and ^1L_b bands were identified as the long axis of the naphthyl unit, while the ^1L_a band was assigned to the short axis of the naphthyl unit. The λ_{max} at 350 nm was expected to arise from the π–π^* transitions of the azo ($N=N$) unit [20]. In the case of **PMRANO$_2$**, a broad peak was observed at approximately 480 nm. This may contribute to the donor–acceptor effect caused by the 4-nitrophenyl group [21]. The CD spectra of the polymers exhibited exciton couplets at 240 nm and 320 nm, which were derived from the ^1B_b and ^1L_b transitions of the BN moiety [22]. We also detected exciton couplets of the azo unit at 340 and 450 nm, which corresponded to the $\pi-\pi^*$ and $n-\pi^*$ transitions, respectively [23].

Irradiation of the polymers at 365 nm induced *trans-cis* photoisomerization of the azo unit (Fig. 2). After photoirradiation for 180 s at 25 °C, the polymers exhibited a photostationary state (PSS). The ratio of the *trans*:*cis* isomers in the PSS was determined to be 60:40 for **PMRAH** and 74:26 for **PMRANO$_2$** using ^{1}H-NMR spectroscopy (Fig. S9). However, recovery of the initial state was achieved after photoirradiation at 436 nm for 180 s or with heat owing to the *cis-trans* back-isomerization.

The temperature dependence of the isomerization behavior was also explored. The photoirradiation duration required to elicit the PSS changed from 180 s to 240 s when

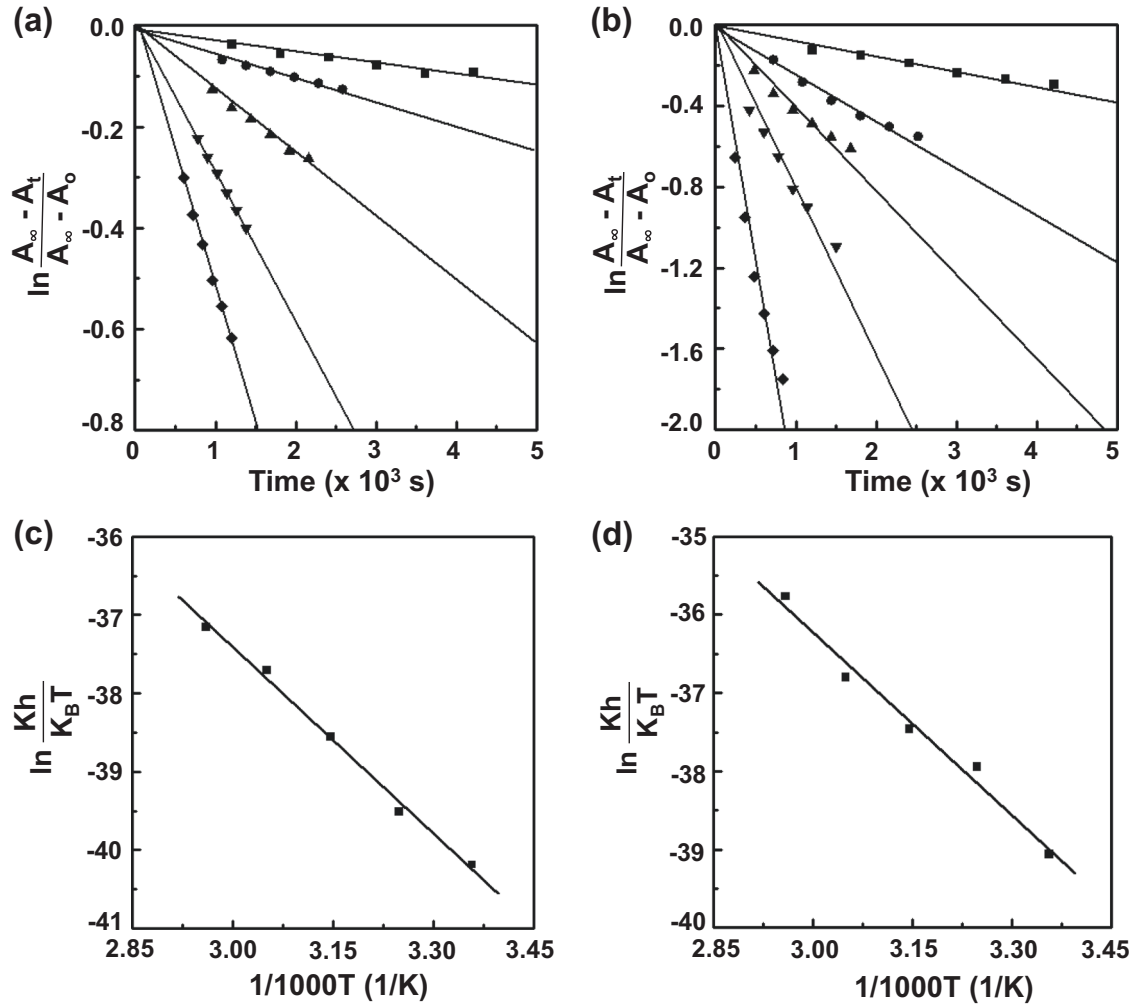

Fig. 3 Kinetics studies of *cis* to *trans* thermal back-isomerization for polymers neat films; (**a**) and (**b**) first-order plots at 25 °C (squares), 35 °C (circles), 45 °C (up triangles), 55 °C (down triangles), and 65 °C (diamonds), (**c**) and (**d**) Eyring plots for **PMRAH** and **PMRANO$_2$** (film thickness = 40 and 30 nm), respectively

Table 2 Kinetic and thermodynamic parameters for the *cis-trans* thermal back-isomerization of the atropisomeric azo polymers

	k at 25 °C ($10^{-5} \times s^{-1}$)	t at 25 °C (h)	t at 65 °C (h)	$\Delta S^{\neq}$ cal mol^{-1} K^{-1}	$\Delta H^{\neq}$ kcal mol^{-1}
PMRAH	2.2	13	0.50	−27	15.8
PMRANO$_2$	6.8	4	0.15	−25	15.5

the temperature was raised from 25 to 65 °C. An acceleration of the *cis-trans* thermal back-isomerization occurred at high temperature, which led to the delayed PSS. The *cis-trans* thermal isomerization of the polymers was described according to the first-order kinetics, similar to that observed for conventional AB moieties [24]. We evaluated the kinetics and thermodynamic parameters for the *cis-trans* thermal back-isomerization at various temperatures, as shown in Fig. 3 and summarized in Table 2. The rate constant was determined by the first-order kinetics equation:

$$\ln \frac{A_\infty - A_t}{A_\infty - A_o} = -kt \quad (1)$$

where A_t, A_0, and A_∞ are the absorbance at 365 nm at time t, initially, and at infinity, respectively. The lifetime (τ: 1/k) of **PMRAH** was 13 h at 25 °C compared with 0.5 h at 65 °C. These results reveal that the *cis-trans* back-isomerization was accelerated by heat owing to the formation of the

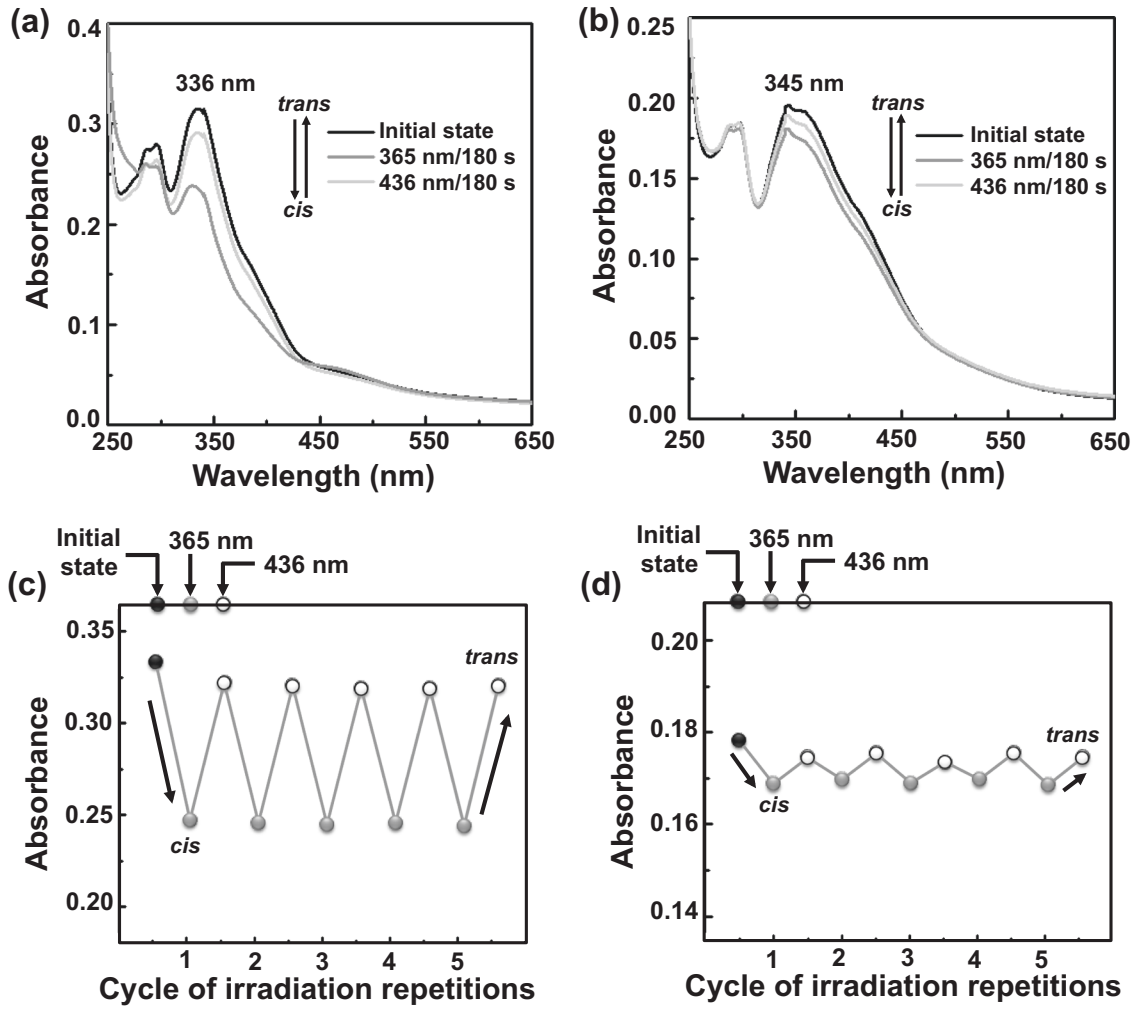

Fig. 4 Photoresponsive behavior of polymers neat films; (**a**) and (**b**) reversible *trans-cis* photoisomerization after UV/Vis light irradiation; (**c**) and (**d**) Switchable behavior of absorption after UV/Vis repetitions cycle of irradiation (180 s, 5 cycles, monitoring wavelengths: 336 and 345 nm) for **PMRAH** and **PMRANO$_2$** (film thickness = 40 and 30 nm), respectively

thermodynamically stable *trans* isomer. Furthermore, **PMRANO$_2$** exhibited fast *cis-trans* back-isomerization, which was three times faster than that of **PMRAH**. The electron-withdrawing nitro group in **PMRANO$_2$** was considered to accelerate the *cis-trans* thermal back-isomerization [25].

The thermodynamic parameters of the enthalpy of activation ($\Delta H^{\neq}$) and entropy of activation ($\Delta S^{\neq}$) were determined according to the Eyring equation: [26]

$$\ln\left(\frac{kh}{k_B T}\right) = -\frac{\Delta H^{\neq}}{RT} + \frac{\Delta S^{\neq}}{R} \quad (2)$$

where R, k_B, and h are the gas, Boltzmann, and Planck constants, respectively. The values of $\Delta S^{\neq}$ and $\Delta H^{\neq}$ were obtained from the intersect and slope, respectively, of the linear plot of $\ln(kh/k_B T)$ versus $1/T$ extrapolated to $T \to \infty$. $\Delta S^{\neq}$ reflects the difference in the degree of freedom between the ground and transition states. The negative values of $\Delta S^{\neq}$ indicated that the *cis-trans* thermal back-isomerization occurred through the inversion mechanism [27].

Chiroptical switching of the atropisomeric azo polymers

As described above, the polymers exhibited reversible *trans-cis* photoisomerization in thin films. Figure 4 shows the reversible change of the polymer films that occurred when alternating photoirradiation at 365 and 436 nm at room temperature. Because the absorbance recovered when the film was irradiated at 436 nm, this photoswitching was ascribed to the *trans-cis* isomerization of the atropisomeric AB unit.

After photoirradiation at 365 nm, the **PMRAH** film showed a change in ellipticity at 240 nm, which corresponded to the ^1B_b transition. This observation arose from the photoinduced molecular twisting motion [28, 29] of the

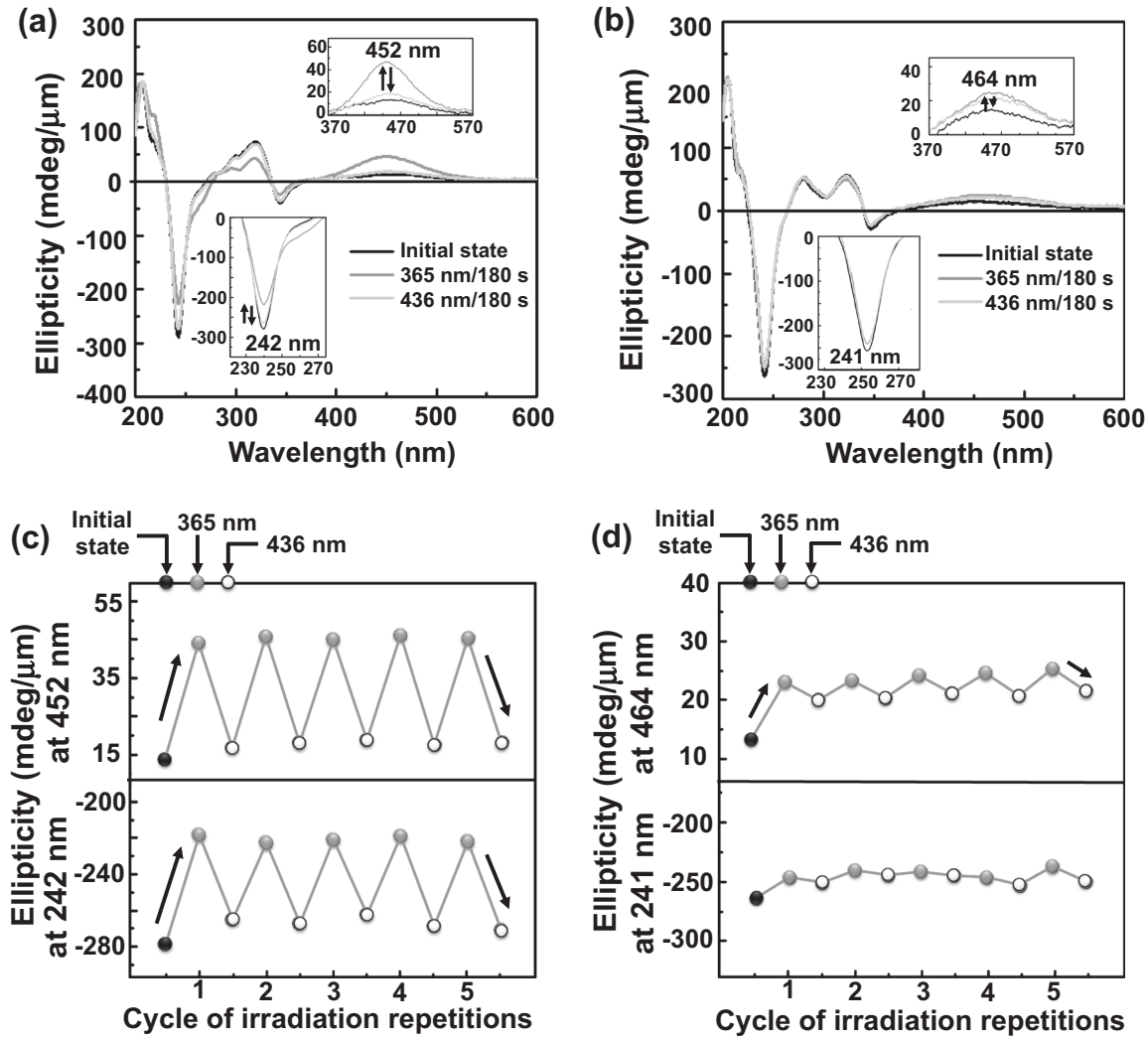

Fig. 5 Chiroptical switching behavior of polymers neat films; (**a**) and (**b**) photo-induced modulation in ellipticity after UV/Vis light irradiation, (**c**) and (**d**) switchable behavior of ellipticity after UV/Vis repetitions cycle of irradiation (180 s, 5 cycles) for **PMRAH** and **PMRANO$_2$** (film thickness = 135 and 120 nm), respectively

BN moiety. Photomodulation of the dihedral angle was estimated to be 21% with an efficient switching behavior of the ellipticities in the case of the **PMRAH** thin film (Fig. 5). The coordinated action of the absorbance and elasticity suggested that the light-driven molecular motion resulted from the change in ellipticity.

Furthermore, the specific optical rotation ($[\alpha]_D^{25}$, c 0.02, THF) of **PMRAH** and **PMRANO$_2$** significantly changed from 255° to 967° and from 138° to 344°, respectively, after irradiation at 365 nm (Fig. S21). A recovery of the initial state could be achieved by irradiation at 436 nm. The same molecular response was investigated in the polymer films, as shown in Fig. 6. The optical rotation of the neat polymer films (α, degree cm^{-1}) switched from 96° to 155° and from 158° to 216° after alternating photoirradiation at 365 and 436 nm for **PMRAH** and **PMRANO$_2$**, respectively.

The $[\alpha]_D^{25}$, α (degree cm^{-1}), ellipticity, and dihedral angle of the atropisomeric **PMRAH** underwent large changes upon UV/Vis irradiation, with efficient reversibility in a neat film, as well as in solutions. Because of these favorable properties, **PMRAH** is regarded as a potential light-driven atropisomeric material for chiroptical switches.

Fluorescence switching induced by photoisomerization

The fluorescence spectra of the polymers show λ_{max} at 409 nm (Fig. S13). Considering the non-radiative relaxation process of *trans*-cis isomerization, AB compounds are non-fluorescent [5, 30]. Based on the molecular design, the BN moiety was determined to act as a fluorescent segment [31], which led to the fluorescence of the investigated polymers.

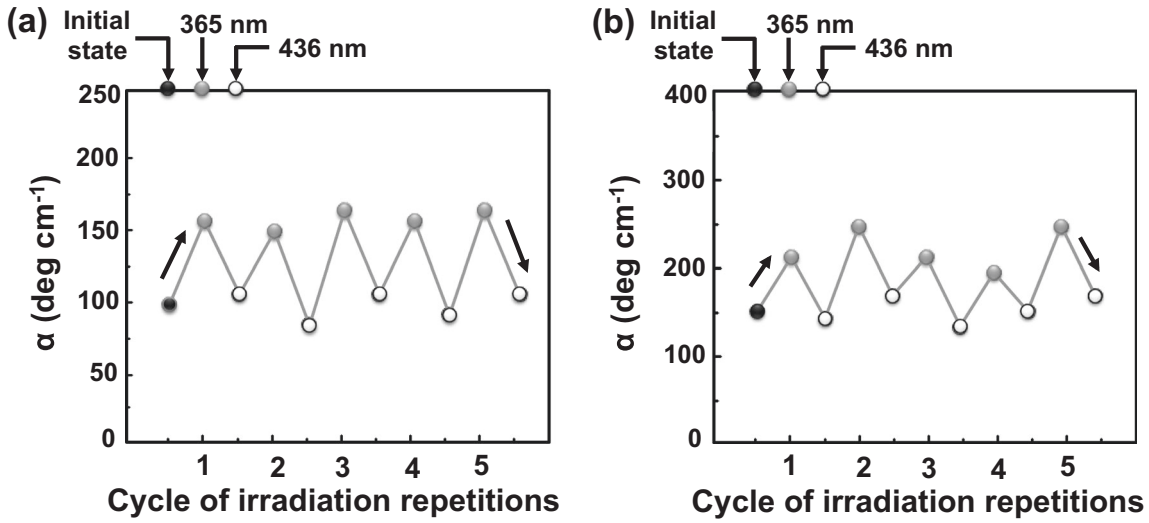

Fig. 6 Chiroptical switching in optical rotations of polymers neat films for **PMRAH** (**a**) and **PMRANO$_2$** (**b**) after UV/Vis repetitions cycle of irradiation (500 s, 5 cycles, monitoring wavelength: 589 nm, film thickness = 135 and 120 nm, respectively)

We observed that the fluorescence spectra of (*R*)-NOBIN under the same conditions exhibited a λ_{max} at 404 nm, which was almost the same λ_{max} as that of the polymers (Fig. S13). Connecting the BN moiety directly to the azo group is considered one of the exceptional methods [32–34] to induce fluorescence emission from AB compounds. The fluorescence quantum yields (Φ_f) were 2.3×10^{-1}, 3.3×10^{-4}, and 1.2×10^{-4} for (*R*)-NOBIN, **PMRAH**, and **PMRANO$_2$**, respectively. These Φ_f values of **PMRAH** and **PMRANO$_2$** were still better than those of the simple azobenzene (10^{-7}) [35].

Interestingly, photoswitchable fluorescence was also obtained; an increase in the fluorescence intensity after irradiation at 365 nm and recovery to the initial state after irradiation at 436 nm was achieved (Fig. S14). A PSS was obtained after irradiation for 180 s for the two states. A switchable fluorescence intensity was obtained after repeated cycles of UV/Vis irradiation, with efficient reversibility (Fig. S15). The Φ_f values of **PMRAH** and **PMRANO$_2$** were also enhanced from 3.3×10^{-4} and 1.2×10^{-4} of the initial state to 4.1×10^{-4} and 1.8×10^{-4}, respectively, after irradiation at 365 nm.

Han et al. [36] also reported an unusual fluorescence enhancement of AB and attributed this enhancement to the light-driven self-assembly of *cis*-AB, which exhibited a sufficient lifetime and a large dipole moment. In our case, the presence of BN is considered to contribute to the enhancement of the dipole moment of *cis*-AB.

Photo-induced change in molecular orientation due to linearly polarized light

The photocontrol of the molecular orientation of the polymers was explored in the film using our four-wave-mixing setup (Scheme S5). A refractive index grating was generated by the irradiation of two linearly polarized pump beams (both in s-polarization). The power of diffraction was measured simultaneously in two polarization states of the probe beam: parallel (s-polarization) and normal (p-polarization) to the direction of the pump beam polarization. We used a near-infrared wavelength (830 nm) for the probe beam, which showed no absorption by our polymer samples. Raman–Nath diffraction, which would lead to a small diffraction, was expected because the sample was thin (several microns). In our system, the insensitive probe beam enabled the detection of a very small diffraction efficiency below 10^{-4}.

We found that the s-polarized probe beam showed high diffraction. After photoirradiation of the neat polymer films (thicknesses of 4.5 and 3.2 μm) using the pump beams, the diffraction power reached approximately 2 and 6 V for **PMRAH** and **PMRANO$_2$**, respectively (Fig. S16). After turning off the laser beam, the diffraction power decreased significantly to approximately 1 and 4 V for **PMRAH** and **PMRANO$_2$**, respectively. These values represent decays of almost 50 and 35% in the diffraction power for **PMRAH** and **PMRANO$_2$**, respectively, after turning off the laser. The photoinduced change in the refractive index (Δn) was evaluated from the diffraction efficiency of the grating according to the following equation [37]:

$$\Delta n \approx \frac{\lambda}{\pi L}\sqrt{\eta} \tag{3}$$

where λ, L, and η are the monitoring wavelength, film thickness, and diffraction efficiency, respectively. The photomodulation of Δn for **PMRAH** and **PMRANO$_2$** was 0.003 and 0.006, respectively, as shown in Fig. 7. The value of Δn for **PMRANO$_2$** was two times higher than that of

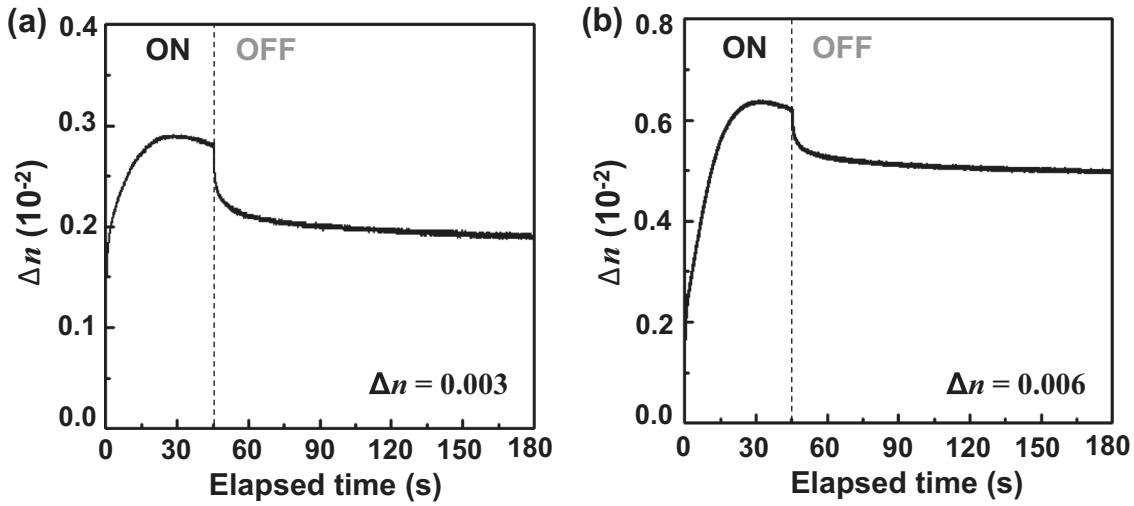

Fig. 7 Photoinduced change in the refractive index of polymers neat films for **PMRAH** (**a**) and **PMRANO$_2$** (**b**). Detection wavelength: 830 nm; film thickness: 4.5 and 3.2 μm, respectively

PMRAH. This difference arose from the effects of the NO_2 chromophore: a) the donor-acceptor effect, which led to the polarizability of the molecules, and b) the photochromic effect, which led to an increase in the absorbance at 532 nm; the corresponding absorption at 532 nm was 0.16 and 0.4 for **PMRAH** and **PMRANO$_2$**, respectively.

However, much lower diffraction was measured by the p-polarization state of the probe beam (Fig. S16). As a result, the diffraction power was approximately 0.5 and 1.0 V for the neat **PMRAH** and **PMRANO$_2$** films, respectively. Such different powers in the two polarization states could be explained by the selective photochromic excitation of AB–BN molecules by the linearly polarized pump beam [38]. The polymer exhibited an initial state in a *trans* form, which has a dominant molecular absorption along the charge-transfer (CT) axis involving an $N=N$ bond. After photoexcitation, the pump beam selectively excited the *trans* form, of which the CT axis was aligned in parallel to the polarization of the pump, which led to selective *trans*-to-*cis* photoisomerization. As a result, the excited *trans* form changed its original molecular orientation, which resulted in optical anisotropy.

Conclusions

We successfully synthesized and characterized light-driven atropisomeric polymers containing AB and BN units in the side chains. The polymers displayed reversible changes in the fluorescence intensities by photoisomerization. The polymers formed a uniform and smooth film and showed reversible *trans-cis* photoisomerization. Additionally, a photoinduced refractive change was observed after photo-irradiation by linearly polarized light. These results suggested that the polymers are potential photoresponsive materials for light-driven molecular switches.

Acknowledgements This work was partially supported by a Grant-in-Aid for Scientific Research (C) (No. 15K05639) for MK from the Ministry of Education, Culture, Sports, Science, and Technology of Japan. We thank Prof. Yu Nagase and Mr. Ryota Ueno of Tokai University for GPC measurements. We acknowledge the Support Unit of Bio-Material Analysis, Research Resources Center, RIKEN Brain Science Institute for the high-resolution mass spectrometry. We are grateful to the Materials Characterization Support Unit, RIKEN Center for Emergent Matter Science (CEMS), for the elemental analysis. We thank Dr. Zhaomin Hou and Dr. Masayoshi Nishiura of the Organometallic Chemistry Laboratory, RIKEN, for the DSC and TGA measurements. We acknowledge Dr. Mikiko Sodeoka and Dr. Yoshihiro Sohtome of the Synthetic Organic Chemistry Laboratory, RIKEN, for the optical rotation measurements. We also thank Dr. Keisuke Tajima and Dr. Kyohei Nakano of the Emergent Functional Polymers Research Team of RIKEN CEMS for the measurements of film thickness. We thank the Edanz Group (www.edanzediting.com/ac) for editing a draft of this manuscript.

Compliance with ethical standards

Conflict of interest The authors declare that they have no conflict of interest.

References

1. Feringa B, Delden R, Wiel M. Chapter 5: Handbook of molecular switches. In: Feringa B, editor. Weinheim, Germany: Wiley-VCH, Verlag GmbH; 2001. pp. 123–63.
2. Koumura N, Zijlstra R, Delden R, Harada N, Feringa B. Light-driven monodirectional molecular rotor. Nature. 1999;401:152–5.
3. Feringa B. In control of motion: from molecular switches to molecular motors. Acc Chem Res. 2001;34:504–13.
4. Browne W, Feringa B. Making molecular machines work. Nat Nanotechnol. 2006;1:25–35.
5. Bandara D, Burdette S. Photoisomerization in different classes of azobenzene. Chem Soc Rev. 2012;41:1809–25.

6. Yu Y, Ikeda T. Alignment modulation of azobenzene-containing liquid crystal systems by photochemical reactions. J Photochem Photobiol C. 2004;5:247–65.
7. Ikeda T. Photomodulation of liquid crystal orientations for photonic applications. J Mater Chem. 2003;13:2037–57.
8. Pu L. Chapter 1: Handbook of 1,1′-Binaphthyl-Based chiral materials. In: Pu L, editor. London, UK: Imperial College Press; 2009. pp. 1–10.
9. Shockravi A, Javadi A, Abouzari-Lotf E. Binaphthyl-based macromolecules: a review. RSC Adv. 2013;3:6717–46.
10. Montbach E, Venkataraman N, Doane J, Khan A, Magyar G, Shiyanovskaya I, Schneider T, Green L, Li Q. Novel optically addressable photochiral displays. Dig Tech Pap Soc Inf Disp Int Symp. 2008;39:919–22.
11. Wang L, Dong H, Li Y, Xue C, Sun L, Yan C, Li Q. Reversible near-infrared light directed reflection in a self-organized helical superstructure loaded with upconversion nanoparticles. J Am Chem Soc. 2014;136:4480–3.
12. Delden R, Mecca T, Rosini C, Feringa B. A chiroptical molecular switch with distinct chiral and photochromic entities and its application in optical switching of a cholesteric liquid crystal. Chem Eur J. 2004;10:61–70.
13. Wang Y, Urbas A, Li Q. Reversible visible-light tuning of self-organized helical superstructures enabled by unprecedented light-driven axially chiral molecular switches. J Am Chem Soc. 2012;134:3342–5.
14. Kawamoto M, Sassa T, Wada T. Photoinduced control over the self-organized orientation of amorphous molecular materials using polarized light. J Phys Chem B. 2010;114:1227–32.
15. Kawamoto M, Shiga N, Takaishi K, Yamashita T. Non-destructive erasable molecular switches and memory using light-driven twisting motions. Chem Commun. 2010;46:8344–6.
16. Takaishi K, Kawamoto M, Tsubaki K, Furuyama T, Muranaka A, Uchiyama M. Chem Eur J. 2011;17:1778–82.
17. Korber K, Tang W, Hu X, Zhang X. A practical synthesis of 2-amino-2′-hydroxy-1,1′-binaphthyl (NOBIN). Tetrahedron Lett. 2002;43:7163–5.
18. Ding K, Wang Y, Yun H, Liu J, Wu Y, Terada M, Okubo Y, Mikami K. Highly efficient and practical optical resolution of 2-amino-2′-hydroxy-1,1′-binaphthyl by molecular complexation with *N*-benzylcinchonidium chloride: a direct transformation to binaphthyl amino phosphine. Chem Eur J. 1999;5:1734–7.
19. Bari L, Pescitelli G, Salvadori P. Conformational study of 2,2′-homosubstituted 1,1′-binaphthyls by means of UV and CD spectroscopy. J Am Chem Soc. 1999;121:7998–8004.
20. Saishoji A, Sato D, Shishido A, Ikeda T. Formation of bragg gratings with large angular multiplicity by means of the photo-induced reorientation of azobenzene copolymers. Langmuir. 2007;23:320–6.
21. Hrozhyk U, Serak S, Tabiryan N, Hoke L, Steeves D, Kimball B, Kedziora G. Systematic study of absorption spectra of donor–acceptor azobenzene mesogenic structures. Mol Cryst Liq Cryst. 2008;489:257–72.
22. Rosini C, Superchi S, Peerlings H, Meijer E. Enantiopure dendrimers derived from the 1,1′-binaphthyl moiety: a correlation between chiroptical properties and conformation of the 1,1′-binaphthyl template. Eur J Org Chem. 2000;2000:61–71.
23. Takaishi K, Muranaka A, Kawamoto M, Uchiyama M. Planar chirality of twisted *trans*-azobenzene structure induced by chiral transfer from binaphthyls. J Org Chem. 2011;76:7623–8.
24. García-Amorós J, Velasco D. Recent advances towards azobenzene-based light- driven real-time information-transmitting materials. Beilstein J Org Chem. 2012;8:1003–17.
25. Mahimwalla Z, Yager K, Mamiya J, Shishido A, Priimagi A, Barrett C. Azobenzene photomechanics: prospects and potential applications. Polym Bull. 2012;69:967–1006.
26. Eyring H. The activated complex and the absolute rate of chemical reactions. Chem Rev. 1935;17:65–77.
27. Liu Z, Morigaki K, Enomoto T, Hashimoto K, Fujishima A. Kinetic studies on the thermal *cis-trans* isomerization of an azo compound in the assembled monolayer film. J Phys Chem. 1992;96:1875–80.
28. Kawamoto M, Aoki T, Wada T. Light-driven twisting behaviour of chiral cyclic compounds. Chem Commun. 2007;0:930–2, http://pubs.rsc.org/en/content/articlelanding/2007/cc/b616320c#!divAbstract.
29. Takaishi K, Kawamoto M, Tsubaki K, Wada T. Photoswitching of dextro/levo rotation with axially chiral binaphthyls linked to an azobenzene. J Org Chem. 2009;74:5723–6.
30. Rau H. Spectroscopic properties of organic azo compounds. Angew Chem, Int Ed. 1973;12:224–35.
31. Pina J, Seixas de Melo J, Burrows H, Macanita A, Galbrecht F, Bunnagel T, Scherf U. Alternating binaphthyl-thiophene copolymers: synthesis, spectroscopy, and photophysics and their relevance to the question of energy migration versus conformational relaxation. Macromolecules. 2009;42:1710–9.
32. Han M, Hara M. Intense fluorescence from light-driven self-assembled aggregates of nonionic azobenzene derivative. J Am Chem Soc. 2005;127:10951–5.
33. Bo Q, Zhao Y. Fluorescence from an azobenzene-containing diblock copolymer micelle in solution. Langmuir. 2007;23:5746–51.
34. Tsai B, Chen C, Hung C, Hsiao V, Chu C. Photoswitchable fluorescence on/off behavior between *cis*- and *trans*-rich azobenzenes. J Mater Chem. 2012;22:20874–7.
35. Fujino T, Arzhantsev S, Tahara T. Femtosecond time-resolved fluorescence study of photoisomerization of *trans*-azobenzene. J Phys Chem A. 2001;105:8123–9.
36. Han M, Hirayama Y, Hara M. Fluorescence enhancement from self-assembled aggregates: substituent effects on self-assembly of azobenzene. Chem Mater. 2006;18:2784–6.
37. Hicher H, Cunther P, Pohl D. Chapter 4: Handbook of laser induced dynamic grating. In: Hicher H, Cunther P, Pohl D, editors. Berlin, Germany: Springer-Verlag; 1986. pp. 94–122.
38. Blanche PA, Lemaire PhC, Maertens C, Dubois P, Jerome R. Polarization holography reveals the nature of the grating in polymers containing azo-dye. Opt Commun. 2000;185:1–12.